Aluminum Bulk Micromachining through an Anodic Oxide Mask by Electrochemical Etching in an Acetic Acid / Perchloric Acid Solution

Tatsuya Kikuchi*, Yuhta Wachi, Masatoshi Sakairi, and Ryosuke O. Suzuki
Faculty of Engineering, Hokkaido University
N13-W8, Kita-ku, Sapporo, Hokkaido, 060-8628, Japan

*Corresponding author: Tatsuya Kikuchi
TEL: +81-11-706-6340
FAX: +81-11-706-6342
E-mail: kiku@eng.hokudai.ac.jp

Abstract

A well-defined microstructure with microchannels and a microchamber was fabricated on an aluminum plate by four steps of a new aluminum bulk micromachining process: anodizing, laser irradiation, electrochemical etching, and ultrasonication. An aluminum specimen was anodized in an oxalic acid solution to form a porous anodic oxide film. The anodized aluminum specimen was irradiated with a pulsed Nd-YAG laser to locally remove the anodic oxide film, and then the exposed aluminum substrate was selectively dissolved by electrochemical etching in an acetic acid / perchloric acid solution. The anodic oxide film showed good insulating properties as a resist mask during electrochemical etching in the solution. A hemicylindrical microgroove with thin free-standing anodic oxide on the groove was fabricated by electrochemical etching, and the groove showed a smooth surface with a calculated mean roughness of 0.2 - 0.3 μm. The free-standing oxides formed by electrochemical etching were easily removed from the specimen by ultrasonication in an ethanol solution. Microchannels 60 μm in diameter and 25 μm in depth connected to a microchamber were successfully fabricated on the aluminum.

Key words: Bulk Micromachining; Aluminum; Anodizing; Electrochemical Etching; Laser Irradiation

1. Introduction

Bulk micromachining of metals and semiconductors has been widely investigated and developed in the fields of electronic devices, micromachining, and nanotechnology [1-5]. Aluminum is generally used for circuit materials, cold plates, and heat sinks due to its low electrical resistivity (2.66 x 10^{-8} Ωm) and high thermal conductivity (237 $Wm^{-1}K^{-1}$) [6], and it is important to develop more precise and smaller bulk micromachining of aluminum for micro- and nano-structure fabrication. The fabrication processes of micro- and nano-meter scale structures are mostly based on photolithography with ultraviolet or X-ray irradiation. However, because photolithography involves many steps with toxic reagents and is seldom applied to materials with three-dimensional structures, a technique for micro- and nano-structure fabrication without photolithography must be developed.

Recently the authors have been developed a novel microstructure fabrication for aluminum and its alloy using laser irradiation and electrochemical techniques [7]. In this technique, an aluminum specimen was anodized in sulfuric, oxalic, and phosphoric acid solutions to form a porous or barrier type anodic oxide film. The oxide film was then irradiated with a pulsed neodymium-doped yttrium aluminum garnet (Nd-YAG) laser to remove the anodic oxide, and a patterned anodic oxide film was fabricated on the aluminum substrate. Here, the anodic oxide acted as a patterned resist mask for microstructure fabrication (Fig. 1). After the laser irradiation, subsequently electro- and electro-less plating caused a selective metal and organic compound deposition on the exposed aluminum substrate, and microstructure fabrication such as micro-coils [8-11], printed circuit boards [12-14], plastic injection molds [15], three-dimensional (3D) complicated micromachine components [16, 17], 3D micro-actuators [18, 19], and electrochemical micro-reactors [20], was successfully achieved.

Aluminum bulk micromachining using patterned anodic oxide can also be realized by electrochemical dissolution of the exposed aluminum substrate. However, electrochemical etching of the exposed aluminum in a sodium chloride solution resulted in uneven electrochemical dissolution [21, 22]; it is difficult to obtain an aluminum microstructure with a flat surface by this process (Fig. 1a). Therefore, a more suitable electrochemical etching solution should be selected for exposed aluminum bulk micromachining with a flat surface. Here, the authors noted that an acetic acid / perchloric acid mixture solution is generally used for the electropolishing solution of aluminum (Fig. 1b). It is a well-known experimental fact that anodic polarization of aluminum in solution causes smoothing of microscopic aluminum surfaces with electrochemical dissolution; however, there have been no reports of the details of the dissolution behavior at a selected area in the solution.

In the present investigation, the authors show a new aluminum bulk micromachining process through an anodic oxide mask by electrochemical etching in an acetic acid / perchloric acid solution. The goal of the current investigation is to describe the optimal conditions for the laser irradiation and electrochemical etching processes and to form

well-defined microchannels with flat surfaces on an aluminum substrate by the developed bulk micromachining.

2. Experimental

2.1 Specimens and pretreatment

Fig. 2 shows a schematic model of the aluminum bulk micromachining through an anodic oxide mask by electrochemical etching in a CH_3COOH / $HClO_4$ solution. The fabrication process consisted of the following four steps: a) aluminum anodizing, b) laser irradiation to remove the anodic oxide, c) electrochemical etching at the laser-irradiated area, and d) ultrasonication to remove free-standing oxides. Highly pure aluminum plates (99.99 wt%, 400 μm thick, Nippon Light Metal Co., Japan) were used as the starting specimens for microstructure fabrication. The specimens were cut into 30 mm x 20 mm pieces with a handle and then ultrasonically degreased in an ethanol solution for 10 min. After degreasing, the specimens were electropolished in a 13.6 M CH_3COOH / 2.56 M $HClO_4$ solution (T = 280 K) with a constant voltage of 28 V for 150 s. The electropolished specimens were anodized in a 0.22 M $(COOH)_2$ solution (T = 293 K) for 3 min with a constant current density of 100 A m^{-2} to form a 1 μm thick porous anodic oxide film on the aluminum substrate (Fig. 2a). A platinum plate was used as the counter electrode, and the solution was stirred with a magnetic mixer during anodizing.

2.2 Laser irradiation for the fabrication of an anodic oxide mask

The anodized specimen was irradiated with a pulsed Nd-YAG laser to fabricate a patterned anodic oxide film on the aluminum substrate (Fig. 2b). The YAG laser (GCR-130-10, Spectra Physics) had a 532 nm wavelength (second harmonic generation), 8 ns pulse width, 10 Hz frequency, and <0.5 mrad beam divergence (full angle). The specimens were immersed in distilled water (T = 295 K) in a cell with stirring and set at the focal position of the laser beam, which passed through an iris diaphragm (Sigma-64, Sigma Koki Co., Japan), a convex lens with a 60 mm focal length (SLQ-15-60P, Sigma Koki Co.), a quartz window, and distilled water. After placement, the specimens were irradiated with the 0.5 mW laser beam to remove the anodic oxide film from the aluminum substrate. During the laser irradiation, the specimens were linearly moved at 12 - 48 μm s^{-1} with an XY-stage (CPC-2DN, Chuo Precision Industrial Co., Japan) controlled by a computer, and a straight line of removed oxide film was fabricated on the specimen by laser irradiation.

2.3 Electrochemical etching through the anodic oxide mask

The laser-irradiated specimens were immersed in 13.6 M CH_3COOH / 2.56 M $HClO_4$ solution (T = 280 K) and then anodically polarized with a constant voltage of 30 V for 30 min to dissolve the aluminum substrate exposed by laser irradiation (Fig. 2c). The applied voltage during electrochemical etching was chosen in reference to previous

investigations [8, 14], and the voltage is a typical value for electrochemical polishing of aluminum. A platinum plate was used as the counter electrode, and the specimens were set in parallel 15 mm from the counter electrode during electrochemical etching. An anodized specimen without laser irradiation was also polarized under the same conditions to examine the electrochemical resistance of anodic oxide as an insulator resist mask. The anodic current density during constant voltage electrolysis was measured by a digital multimeter connected to a PC system.

After the electrochemical etching, free-standing oxides formed on the groove by the electrochemical etching were removed by ultrasonication in ethanol for 15 min (Fig. 2d). Microchannel patterns with well-defined microgrooves were also fabricated on the aluminum plate by the process shown in Fig. 2. Structural changes of the specimen on each step were examined by scanning electron microscopy (SEM, Miniscope TM-1000, Hitachi) and confocal scanning laser microscopy (CSLM, 1SA21, Lasertec).

3. Results and discussion

Aluminum specimens covered with a 1 μm thick anodic oxide film were irradiated with the YAG laser to remove the anodic oxide. Fig. 3a shows an SEM image of the surface of a specimen irradiated linearly with the 0.5 mW laser at a scanning rate of 48 μm s^{-1}. In the figure, the gray line at the center corresponds to the laser-irradiated area, and the dark gray parts around the line correspond to the anodic oxide film that was not laser irradiated. It can be seen that the anodic oxide film was removed linearly and the exposed aluminum substrate had an uneven surface due to rapid melting and solidification of the aluminum by the laser ablation. There was no crack in the anodic oxide near the film-removed line; however, the width of the line was periodically changed due to the fast scanning of the circular laser beam. Fig. 3b shows an SEM image of the oxide-removed line formed by laser irradiation at v = 12 μm s^{-1} and under the same energy shown in Fig. 3a. It is clear that a microgroove with a relatively straight contour was obtained by the slow scanning of the laser beam, while the exposed aluminum substrate also shows an uneven surface.

As mentioned previously, in the fabrication method used in this work, the non-irradiated areas of the anodic oxide films acted as insulating resist masks during the electrochemical etching (Fig. 2c). Therefore, the electrochemical resistance of the anodic oxide film was examined to determine the optimal conditions for electrochemical etching. Fig. 4 shows the relationship between the anodic current density, i, and the cell voltage, V, for a 1 μm thick anodized specimen without laser irradiation and under anodic polarization in a 13.6 M CH_3COOH / 2.56 M $HClO_4$ solution (280 K). Here, the anodic current density corresponds to the amount of aluminum dissolution that through the imperfections and reached the aluminum substrate after penetration of the solution via the following equation:

$$Al = Al^{3+} + 3e^- \quad (1)$$

It is clear from Fig. 4 that no current was observed in the initial period until V = 44 V.

After the initial period, the current density increased rapidly at V = 48 V after slightly increasing with the cell voltage between the range of 44 - 48 V. Then, the current density gradually decreased with increasing cell voltage. This current behavior suggests that the aluminum easily dissolved through the anodic oxide film at cell voltages of 48 V and above. Conversely, under anodic polarization, the anodic oxide showed good insulating properties until 44 V was reached in the solution.

The porous anodic oxide film that formed on the aluminum consisted of numerous fine hexagonal cells perpendicular to the aluminum substrate, and each cell had a pore at the center [23-26]. The pores were separated from the aluminum substrate by a thin hemispherical “barrier layer”, existing at the interface between the porous layer and the aluminum substrate (see insert figure). In this investigation, the barrier layer had a dielectric strength of 48 V because the applied voltage measured approximately 48 V during anodizing under a constant current density. However, the barrier layer in the oxide film formed by the anodizing had many imperfections, and the electrochemical dissolution of the aluminum may have occurred through the imperfections below the voltage of 48 V. Therefore, a slight current density of the electrochemical dissolution was measured in the range of 44 - 48 V, as shown in Fig. 4. The current density decreasing after the maximum value may have been due to diffusion limitations of the electrolytes under anodic polarization. For aluminum bulk micromachining through the patterned anodic oxide mask, electrochemical etching was carried out at a constant voltage of 30 V because the anodic oxide had sufficient dielectric strength under this etching condition.

Fig. 5 shows SEM images of the surfaces of electroetched specimens through the anodic oxide mask, shown in Fig. 3b, at a constant voltage of 30 V for a) 2 min, b) 5 min, and c) 30 min. The electrochemical etching led to the electrochemical dissolution of the aluminum substrate at the laser-irradiated area, and the aluminum substrates electro-etched for 2 min and 5 min showed flat surfaces compared with Fig. 3b. On the other hand, the bottom of the exposed aluminum shown in Fig. 5c was not observed due to the formation of a deep groove caused by the longer electrochemical etching. In addition, the electrochemical etching resulted in an undercutting (light-gray parts around the groove in each figure) formed by the isotropic dissolution of aluminum under the oxide film near the laser-irradiated area. The width of these free-standing oxide films increased as the electroetching time increased, and the undulations of the edge of the groove became uniform along the groove length as the electroetching time increased.

Time variations in the calculated mean roughness by CSLM measurements, R_a, of the groove bottom formed by the electrochemical etching of laser-irradiated specimens are shown in Fig. 6. The roughness of the laser-irradiated specimen was 1.04 μm due to the uneven surface, shown in Fig. 3b, formed by laser ablation. In fact, the two-dimensional depth profile of the resulting groove shows an approximately 10 μm difference in elevation (see insert figure a). The roughness decreased rapidly at the

initial stage of electrochemical etching and then reached a steady value of approximately 0.2 μm. The depth profile of the etched specimen for 2 min shows a flat surface within 1 μm difference in elevation (insert figure b), and it is clear that microgrooves with a flat surface can be obtained by electrochemical etching.

Electrochemical etching of aluminum in a CH_3COOH / $HClO_4$ solution resulted in microsmoothing of the surface with electrochemical dissolution [27, 28]. The aluminum substrate rapidly dissolved into the solution in the initial stage of electrochemical etching, and a high concentrated dissolved-electrolyte layer was formed on the aluminum surface during etching. Under these electrochemical mass-transport limitations, micrometer-scale convex parts on the surface preferentially dissolved into the solution after the initial stage. Therefore, the aluminum surface exposed by the laser irradiation was smoothed by electrochemical etching at the micro-level. Moreover, the exposed aluminum dissolved isotropically from the local opening by electrochemical etching at the macro-level, and a hemicylindrical aluminum groove with a flat surface was formed on the aluminum substrate.

Fig. 7 shows the changes in a) the width of the groove, W, and b) the depth of the groove, D, with the electrochemical etching time, t_e. Both the width and depth of the groove increased with electrochemical etching time, and the increasing rate of the width slightly decreased with the etching time, whereas the depth increased linearly. This asymmetry dissolution effect has already been reported in experiments and a simulation of electrochemical bulk micromachining with a photoresist mask [29]. In this report, the opening of the resist mask was smaller than the final groove width due to undercutting, similar to our experiments. The reason may be that the size of the groove was too small, as it was on the same order as the diffusion layer thickness. In fact, the changes of the grooves obtained by Fig. 7 agree with the experimentally measured and simulated etched profiles reported in the investigation [29]. It is noted again that the width and depth of the grooves formed by electrochemical etching increased with the etching time, as shown in Fig. 7, thus allowing for precise size control.

Fig. 8 shows SEM images of the surface of the electroetched specimens at a constant voltage of 30 V for a) 2 min, b) 5 min, and c) 30 min after laser irradiation under the fast scanning rate, as shown in Fig. 3a. The anodic oxide film was incompletely removed from the aluminum substrate by the laser irradiation because the scanning rate of the laser beam was too high, and an accordingly irregular-shaped microgroove with free-standing oxides was formed on the aluminum substrate by the electrochemical etching (Figs. 8a and 8b). However, it is clear from Fig. 8c that the longer electrochemical etching caused the formation of a groove with relatively straight contour, similar to Fig. 5c (see the light-gray parts formed by the undercutting). Comparing Fig. 8c with Fig. 5c, the size and linearity of the microgrooves, shown by the light-gray color, were almost the same, although the shapes of the free-standing oxides formed by electrochemical etching were widely different. This characteristic dissolution phenomenon was only observed after electrochemical etching with

microsmoothing effects. Therefore, the slightly irregular shape of the anodic oxide mask formed by laser irradiation had no effect on the formation of the microgroove with straight contours on the aluminum substrate.

Electrochemical etching of the laser-irradiated specimen enabled the formation of microgrooves with free-standing anodic oxide on the aluminum substrate, as shown in Figs. 5 and 8. This free-standing oxide on the groove can be mechanically removed by ultrasonication. Fig. 9 shows SEM images of the a) surface and b) cross-section of the microgroove after ultrasonication in ethanol for 15 min, where the microgroove was fabricated by laser irradiation and electrochemical etching, as shown in Fig. 5c. Here, a crevasse was formed at the interface between the aluminum substrate and epoxy resin (Fig. 9b). It can be seen that the free-standing anodic oxides around the laser-irradiated area were completely removed, although some needle-shaped oxides were observed in the edges of the groove (Fig. 9a). This incomplete removal of the free-standing anodic oxide, however, is permitted for microchannel applications because the fluids flowing in the microgrooves are hardly affected by the remaining oxides on the outermost part. In addition, the anodic oxide can be completely dissolved from the aluminum substrate by immersion in a CrO_3 / H_3PO_4 solution, although the solution involves hexavalent chromium ions, and the usage of the solution is discouraged for the anodic oxide removal. A semicircular microgroove was observed from Fig. 9b, and it is clear that isotropic electrochemical etching was occurred during electrochemical etching, shown in Fig. 1b.

Fig. 10 shows SEM images of the microchannel pattern fabricated by anodizing, laser irradiation, electrochemical etching, and free-standing oxide removal, as shown in Fig. 2. During the microfabrication, the aluminum specimen covered with anodic oxide (1 μm thick) was irradiated with the laser continuously and then electroetched in a CH_3COOH / $HClO_4$ solution for 30 min to form microgrooves and a microchamber on the aluminum substrate before ultrasonication. In these figures, the light-gray parts correspond to the aluminum substrate, and the black parts correspond to the anodic oxide film on the aluminum. Here, the anodic oxide had a linear striped pattern (Figs. 10a and 10b), formed by hot rolling, for aluminum plate production. The micropattern consisted of microchannels 60 μm in diameter and 25 μm in depth and connected with the microchamber at the center. It is clear from Fig. 10 that the microchannels had good definition with a smooth inner surface, and the anodic oxide films can be observed on the aluminum substrate around the microchannels (Fig. 10c). The edge of the anodic oxide showed a slightly irregular shape due to the mechanical removal by ultrasonication, as shown in Fig. 9. These microchannels can be applied to microdevices such as heat sinks, cold plates, and so on. Moreover, formation of an anodic oxide film on the entire surface by further anodizing improves the corrosion resistance of the fabricated pattern.

In summary, well-defined microchannels were fabricated on an aluminum surface by selective anodic dissolution in a CH_3COOH / $HClO_4$ solution through an anodic oxide

mask. More precise and smaller oxide micropatterns can be fabricated by laser irradiation with a high focusing optical system under optimal conditions [12]. In addition, the process in this investigation can be simply applied to microstructure fabrication on three-dimensional substrates with curved and stepped surfaces, which have been developed in previous work [16, 17]. On the other hand, the process may not be suitable for bulk micromachining with large-scale materials since laser processing is a relatively slow fabrication method. In order to solve the problem, increasing of the laser frequency and scanning rate during laser irradiation is required. The fabrication technique described above can be applied to other valve metals including titanium, zirconium, hafnium, tantalum, niobium, and so on. Here, it is important to understand the chemical stability of anodic oxides formed on these metal substrates in electrochemical etching solutions. Subsequently, laser irradiation and electrochemical etching under the optimal conditions enable micromachining on these metal substrates.

4. Conclusions

This investigation demonstrated a new aluminum bulk micromachining process by anodizing, laser irradiation, and electrochemical etching in an acetic acid / perchloric acid solution, and the following conclusions may be drawn from the investigation.

Electrochemical etching in an acetic acid / perchloric acid solution through an anodic oxide mask enables the fabrication of microgrooves with free-standing oxides on an aluminum substrate, and the width and depth of the grooves are determined by the electrochemical etching time. During electrochemical etching, the anodic oxide film formed by anodizing has good insulating properties in the solution. The free-standing oxides by the etching are easily removed from the specimen by ultrasonication. A microstructure consisting of microchannels 60 μm in diameter and 25 μm in depth and connected with a microchamber can be successfully fabricated by aluminum bulk micromachining.

Acknowledgements

This work was financially supported partially by a research grant from The Murata Science Foundation (Nagaokakyo, Kyoto, Japan), Hokkaido Gas Co. (Sapporo, Hokkaido, Japan), and the Japan Society for the Promotion of Science (JSPS) “KAKENHI”. The authors also thank Dr. Ken Ebihara (Nippon Light Metal Co., Japan) for supplying the highly pure aluminum plates.

References

1) J. Y. Kim, O. J. Kwon, S. M. Hwang, M. S. Kang, J. J. Kim, J. Power Sources 161 (2006) 432-436.
2) S. J. Lee, A. Chang-Chien, S. W. Cha, R. O’Hayre, Y. I. Park, Y. Saito, F. B. Prinz, J. Power Sources 112 (2002) 410-418.
3) D. Bogojevic, K. Sefiane, A. J. Walton, H. Lin, G. Cummins, Int. J. Heat and Fluid

Flow 30 (2009) 854-867.
4) P. Dixit, N. Lin, J. Miao, W. K. Wong, T. K. Choon, Sens. Actuat. A 141 (2008) 685-694.
5) D. Landolt, J. Electrochem. Soc. 149 (2002) S9-S20.
6) R. Kubo, S. Nagakura, H. Iguchi, H. Ezawa, Rikagaku-Jiten 4th edition, Iwanami Shoten, Tokyo, Japan, 1992.
7) T. Kikuchi, S. Z. Chu, S. Jonishi, M. Sakairi, H. Takahashi, Electrochim. Acta 47 (2001) 225-234.
8) S. Z. Chu, M. Sakairi, H. Takahashi, Z. X. Qui, J. Electrochem. Soc. 146 (1999) 537-546.
9) S. Z. Chu, M. Sakairi, I. Saeki, H. Takahashi, J. Electrochem. Soc. 146 (1999) 2876-2885.
10) S. Z. Chu, M. Sakairi, H. Takahashi, J. Electrochem. Soc. 147 (2000) 1423-1434.
11) S. Z. Chu, M. Sakairi, H. Takahashi, K. Shimamura, Y. Abe, J. Electrochem. Soc. 147 (2000) 2181-2189.
12) T. Kikuchi, M. Sakairi, H. Takahashi, Y. Abe, N. Katayama, Surf. Coat. Technol. 169-170C (2003) 199-202.
13) H. Jha, T. Kikuchi, M. Sakairi, H. Takahashi, ACS Appl. Mater. Interfaces 2 (2010) 774-777.
14) T. Kikuchi, M. Sakairi, H. Takahashi, Electrochim. Acta 54 (2009) 7018-7024.
15) S. M. Moon, M. Sakairi, H. Takahashi, K. Shimamura, Electrochemistry 71 (2003) 260-265.
16) T. Kikuchi, M. Sakairi, H. Takahashi, J. Electrochem. Soc. 150 (2003) C567-C572.
17) T. Kikuchi, H. Takahashi, T. Maruko, Electrochim. Acta 52 (2007) 2352-2358.
18) Y. Akiyama, T. Kikuchi, M. Ueda, M. Iida, M. Sakairi, H. Takahashi, Electrochim. Acta 51 (2006) 4834-4840.
19) T. Kikuchi, Y. Akiyama, M. Ueda, M. Sakairi, H. Takahashi, Electrochim. Acta 52 (2007) 4480-4486.
20) M. Sakairi, M. Yamada, T. Kikuchi, H. Takahashi, Electrochim. Acta 52 (2007) 6268-6274.
21) T. Kikuchi, M. Sakairi, H. Takahashi, Y. Abe, N. Katayama, J. Electrochem. Soc. 148 (2001) C740-C745.
22) T. Kikuchi, H. Takahashi, T. Maruko, J. Suf. Fin. Soc. Jpn. 56 (2005) 409-414.
23) M. Nagayama, K. Tamura, H. Takahashi, Corr. Sci. 12 (1972) 133-136.
24) H. Takahashi, M. Nagayama, H. Akahori, and A. Kitahara, J. Electron Microscopy 22 (1973) 149-157.
25) S. Ono, M. Saito, M. Ishiguro, H. Asoh, J. Electrochem. Soc. 151 (2004) B473-B478.
26) K. R. Hebert, S. P. Albu, I. Paramasivam, P. Schmuki, Nature Mater. 11 (2012) 162-166.
27) P. A. Jacquet, Nature 135 (1935) 1076.

28) D. Landolt, Electrochim. Acta 32 (1987) 1-11.
29) C. Madore, O. Piotrowski, D. Landolt, J. Electrochem. Soc. 146 (1999) 2526-2532.

Captions

Fig. 1 Schematic models of electrochemical etching through an anodic oxide mask on aluminum in a) sodium chloride and b) acetic acid / perchloric acid solutions.

Fig. 2 Schematic model for aluminum bulk micromachining: a) Anodizing to form a porous anodic oxide film, b) laser irradiation to linearly remove the anodic oxide film, c) electrochemical etching at the laser-irradiated area, and d) ultrasonication to remove free-standing oxides on the groove.

Fig. 3 SEM images of the surface of the laser-irradiated specimen at a scanning rate of v = a) 48 μm s^{-1} and b) 12 μm s^{-1} with a 0.5 mW laser. Anodic oxide films with a 1 μm thickness were formed on the aluminum substrate before laser irradiation.

Fig. 4 Change in anodic current density, i, with cell voltage, V, in a 13.6 M CH_3COOH / 2.56 M $HClO_4$ solution at 280 K using an aluminum specimen covered with a 1 μm thick porous anodic oxide film. The insert figure shows schematic model of the porous oxide film.

Fig. 5 SEM images of the microgroove fabricated by electrochemical etching in CH_3COOH / $HClO_4$ solution for a) 2 min, b) 5 min, and c) 30 min after laser irradiation. The laser-irradiated specimen shown in Fig. 3b was used for electrochemical etching.

Fig. 6 Change in calculated mean roughness at the etched surface, R_a, with electrochemical etching time, t_e. The insert figure shows CSLM two-dimensional depth profiles at the surface, which is parallel to the longitudinal direction of the laser-irradiated area.

Fig. 7 Change in a) groove width, W, and b) groove depth, D, with electrochemical etching time, t_e, in a CH_3COOH / $HClO_4$ solution.

Fig. 8 SEM images of the surface of the etched specimen in a CH_3COOH / $HClO_4$ solution for a) 2 min, b) 5 min, and c) 30 min after laser irradiation shown in Fig. 3a.

Fig. 9 SEM images of the a) surface and b) cross-section of the microgroove fabricated on the aluminum specimen after ultrasonication for 15 min. The conditions for electrochemical etching are shown in Fig. 5c.

Fig. 10 SEM images of microchannels connected with a microchamber on aluminum, which was fabricated by successive procedures of anodizing, laser irradiation, electrochemical etching, and free-standing oxide removal. The microchannels are 60 μm

in width.

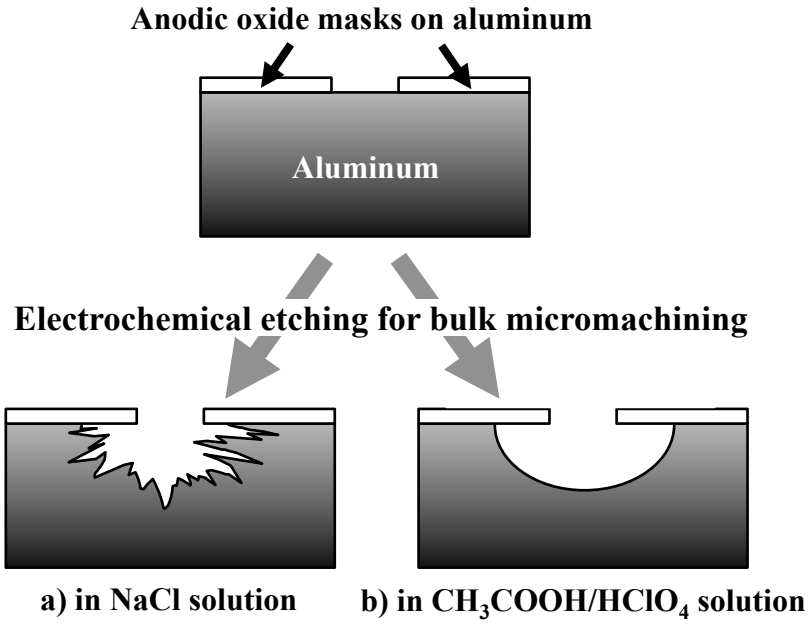
Anodic oxide masks on aluminum
Aluminum
Electrochemical etching for bulk micromachining
a) in NaCl solution
b) in $CH_3COOH/HClO_4$ solution

Fig. 1

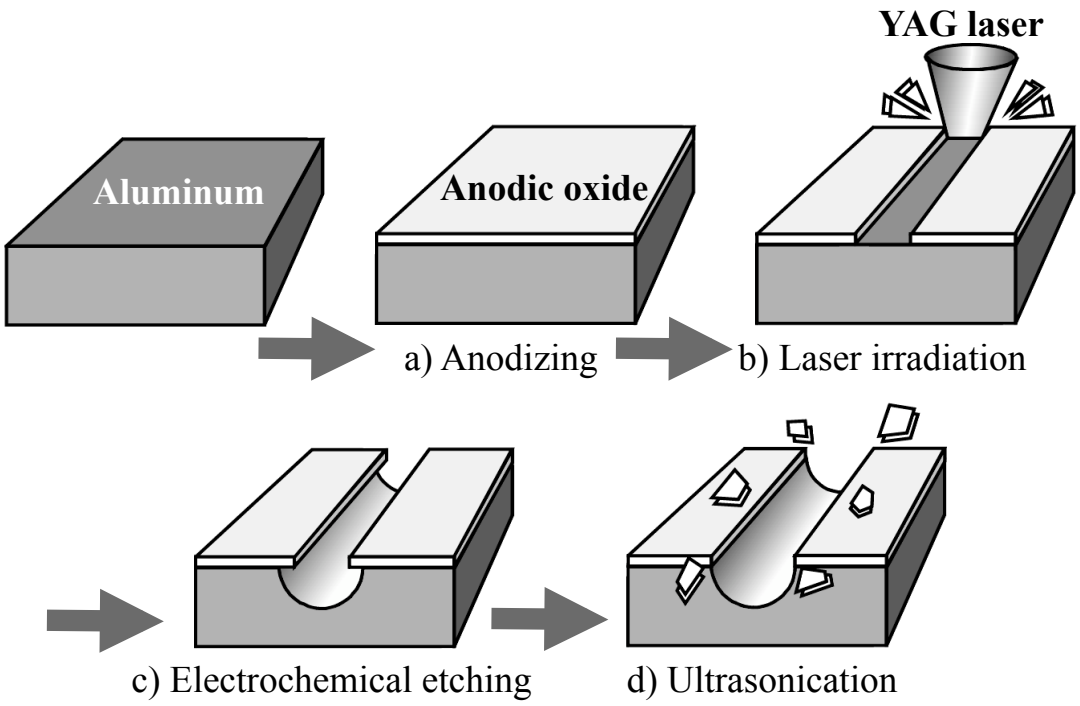
YAG laser
Aluminum
Anodic oxide
a) Anodizing
b) Laser irradiation
c) Electrochemical etching
d) Ultrasonication

Fig. 2

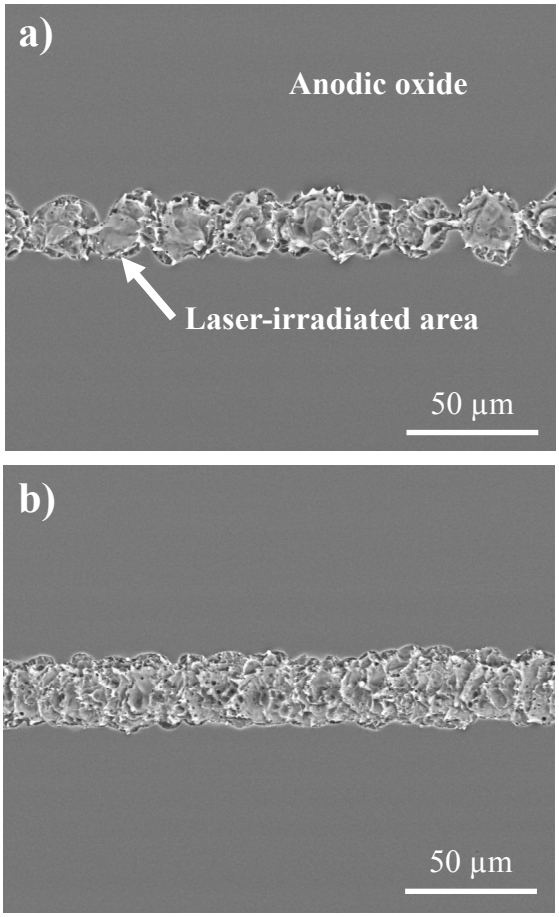

Fig. 3

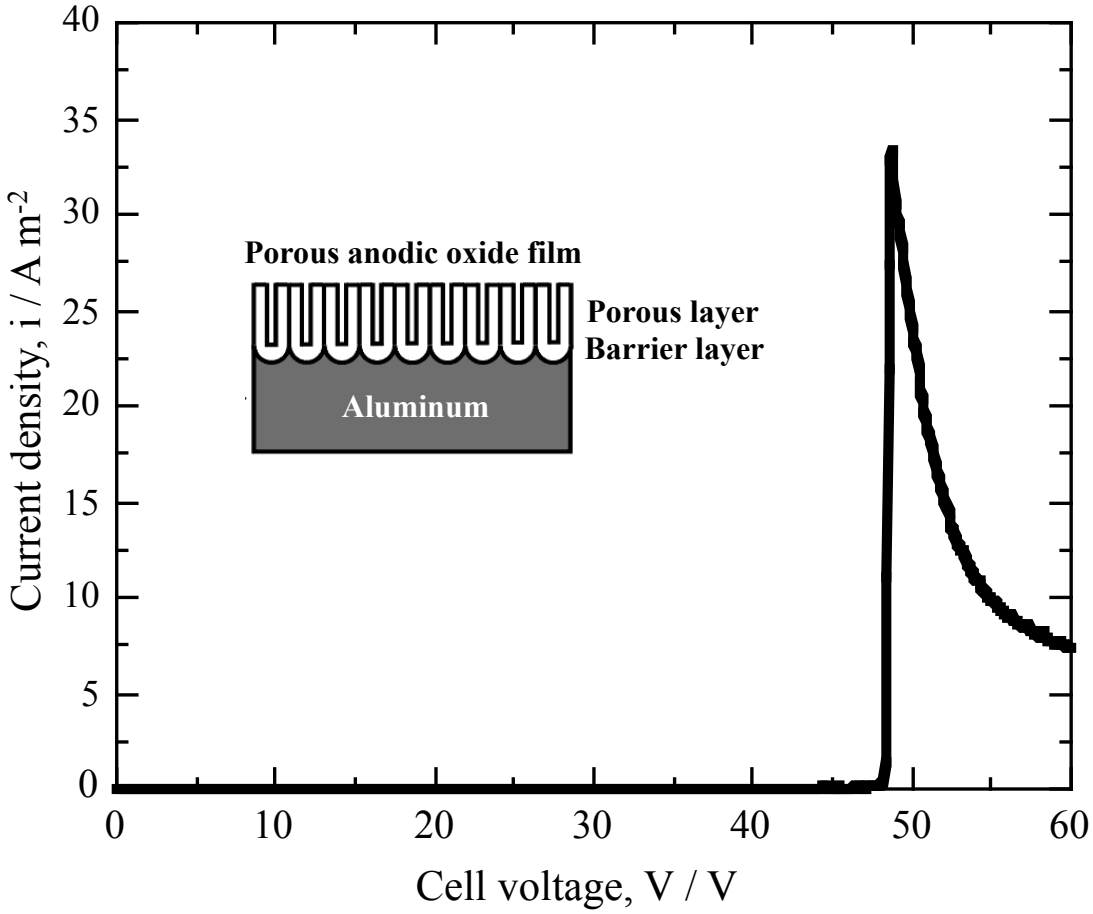
Current density, i / A m-2
Cell voltage, V / V
Porous anodic oxide film
Porous layer
Barrier layer
Aluminum
0
5
10
15
20
25
30
35
40
0
10
20
30
40
50
60

Fig. 4

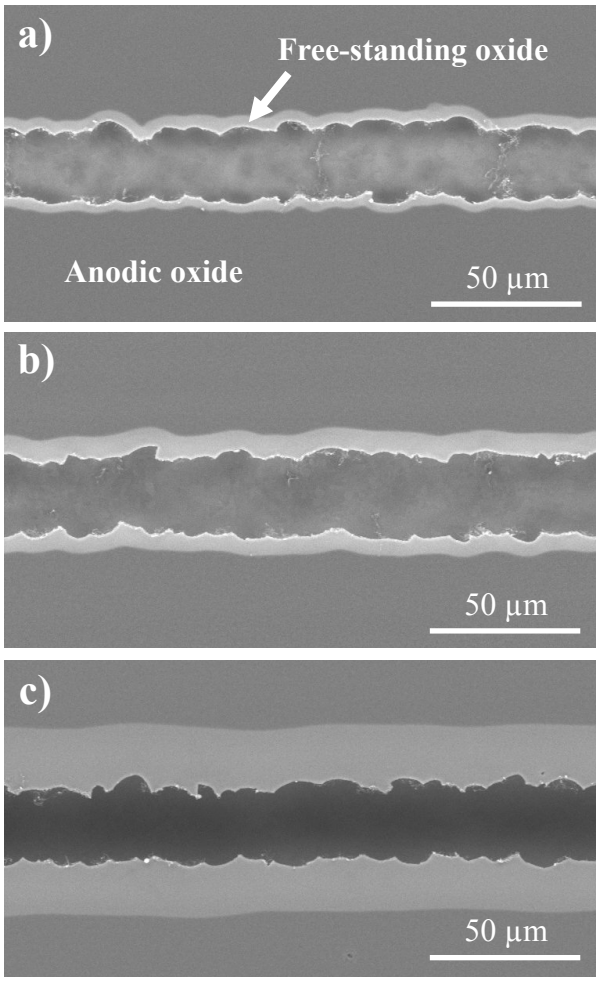

Fig. 5

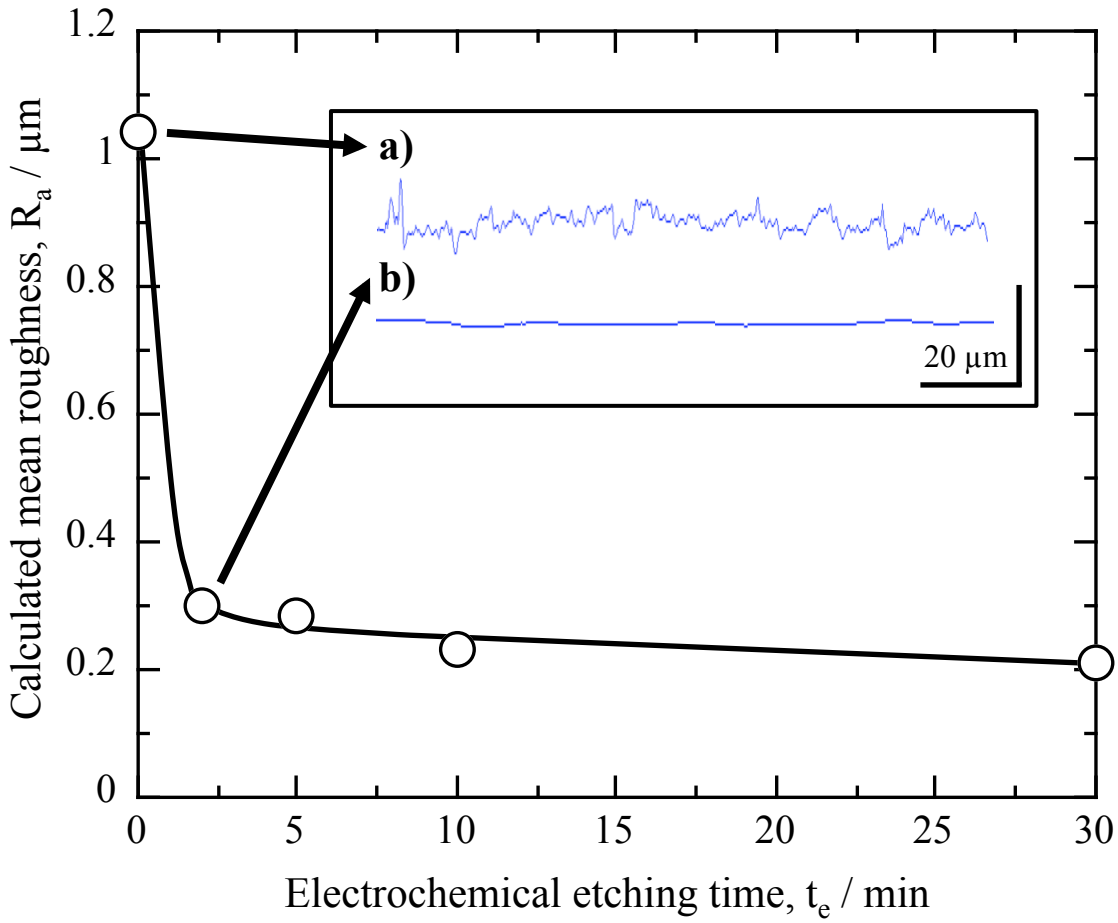
1.2
1
0.8
0.6
0.4
0.2
0
0
5
10
15
20
25
30
Calculated mean roughness, R_a / µm
Electrochemical etching time, t_e / min
a)
b)
20 µm

Fig. 6

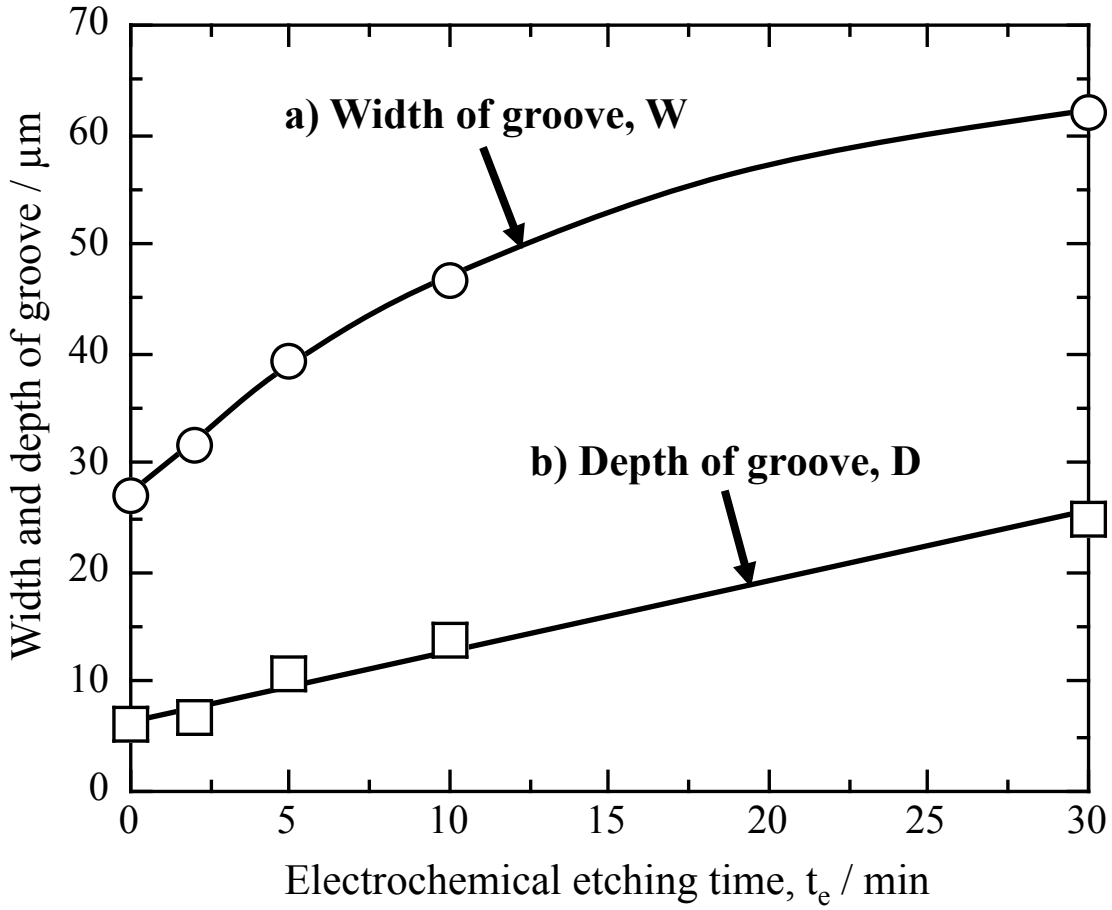
a) Width of groove, W
b) Depth of groove, D
Width and depth of groove / μm
Electrochemical etching time, t_e / min
0
10
20
30
40
50
60
70
0
5
10
15
20
25
30

Fig. 7

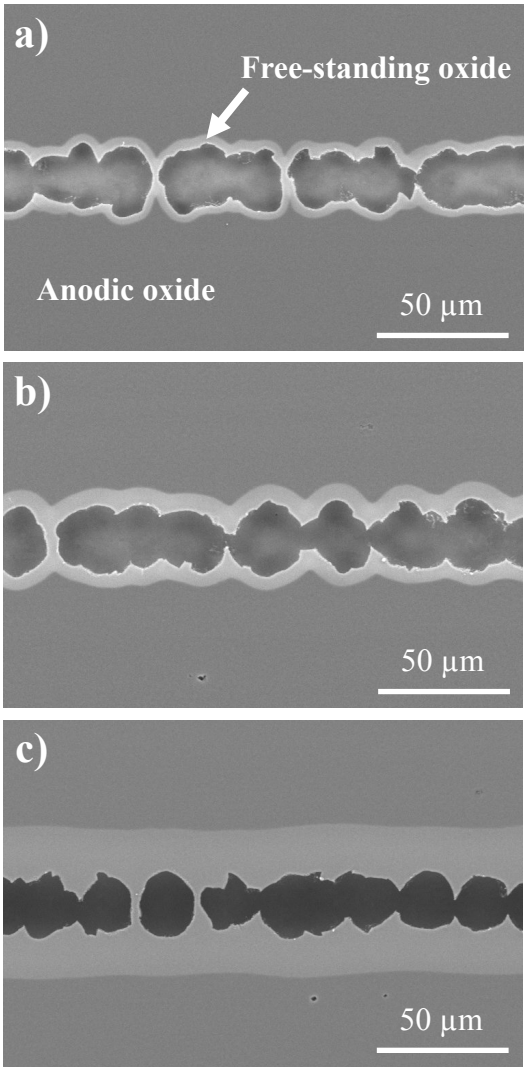

Fig. 8

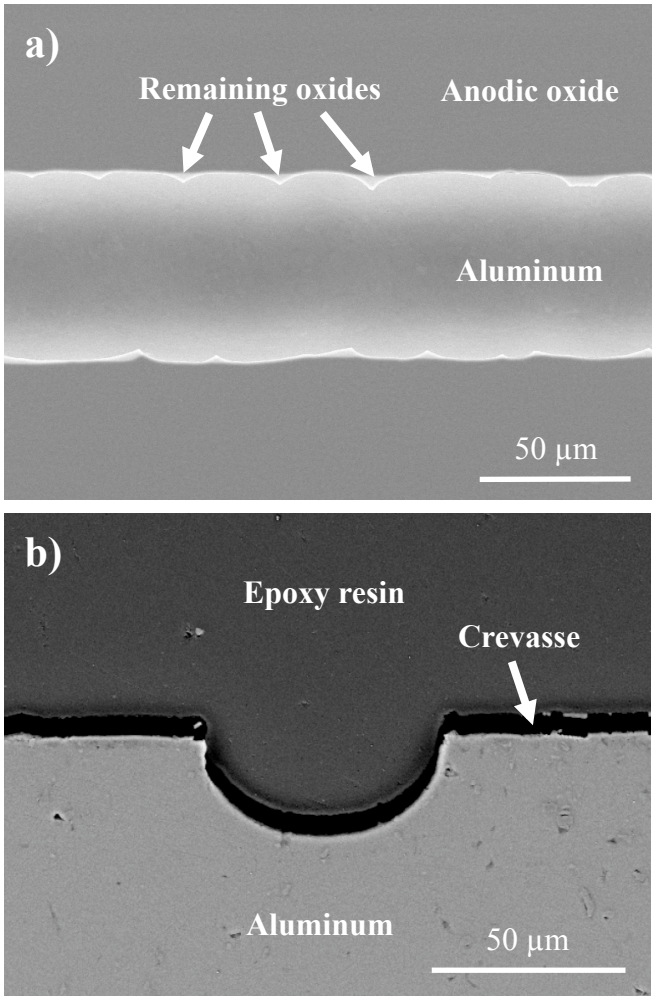
a)
Remaining oxides
Anodic oxide
Aluminum
50 µm
b)
Epoxy resin
Crevasse
Aluminum
50 µm

Fig. 9

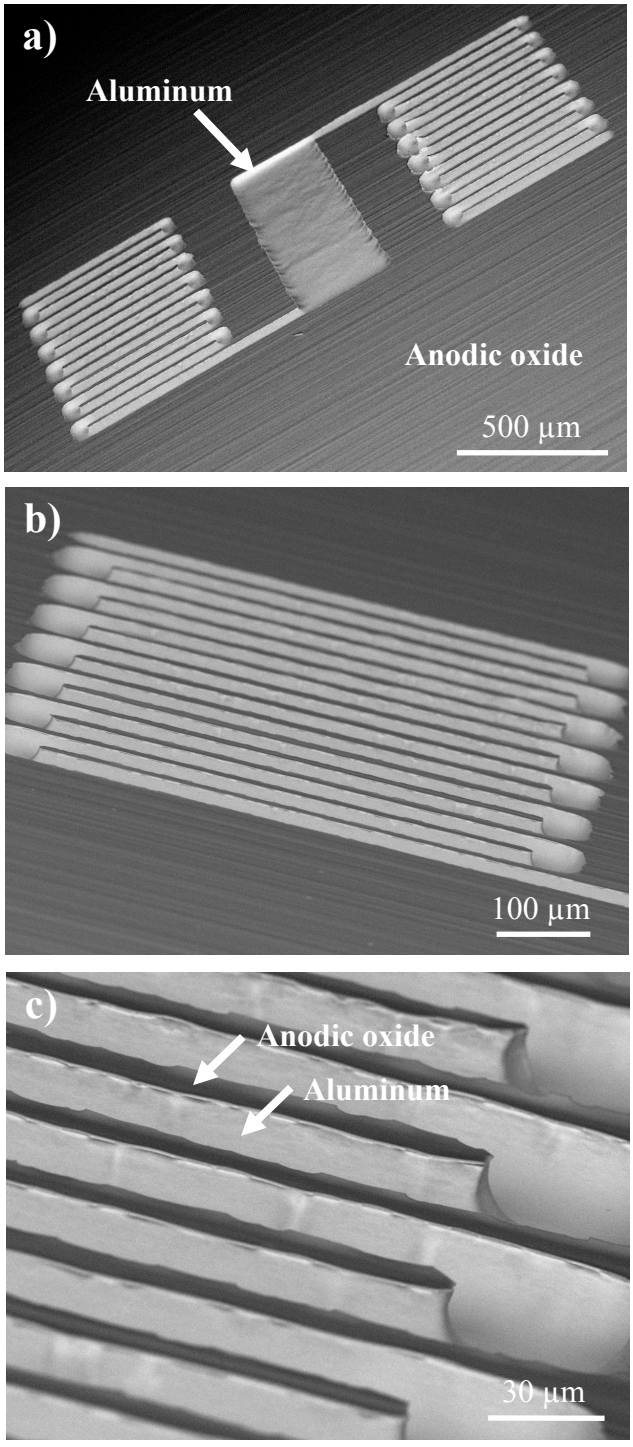
a)
Aluminum
Anodic oxide
500 µm
b)
100 µm
c)
Anodic oxide
Aluminum
30 µm

Fig. 10